

****FULL TITLE****
*ASP Conference Series, Vol. **VOLUME**, **YEAR OF PUBLICATION***
****NAMES OF EDITORS****

3D MHD Simulations of Disk Accretion onto Magnetized Stars: Numerical Approach and Sample Simulations

Marina M. Romanova¹, Alexander V. Koldoba², Galina V. Ustyugova³,
 Akshay K. Kulkarni¹, Min Long⁴, Richard V.E. Lovelace¹

Abstract. We present results of global 3D MHD simulations of disk accretion to a rotating star with dipole and more complex magnetic fields using a Godunov-type code based on the “cubed sphere” grid developed earlier in our group. We describe the code and the grid and show examples of simulation results.

1. Introduction

A wide range of stars have significant intrinsic magnetic fields. Stars are usually strongly magnetized during the protostellar stage (T Tauri stars), and after collapse to a white dwarf or a neutron star. Many observational properties of these stars are determined by the interaction of the accreting disk matter with the rotating magnetosphere of the star (see e.g., Bouvier et al. 2007 for review). In general, the magnetic axis of the star does not coincide with the rotational axis, due to which the magnetospheric flow is complicated and the problem requires global 3D MHD simulations. In addition, the magnetic field of the star may have a complex structure, which adds complications and the necessity to consider this problem in a global MHD approach.

To solve this problem we developed a special 3D MHD code on the cubed sphere grid (Koldoba et al. 2002, see also Putman & Lin 2007) which is somewhat similar to Yin-Yang grid (Kageyama and Sato 2004). This grid has a number of advantages over spherical or Cartesian grids. A “cubed sphere” grid had been originally developed for the surface of a sphere for geophysical applications (Sadourny 1972; Ronchi, Iacono, & Paolucci 1996). In contrast with these authors, we perform simulations in three-dimensional space. We used a Godunov-type numerical scheme (Powell et al. 1999; Kulikowskii, Pogorelov, & Semenov 2001) and were able to perform pioneering simulations of disk accretion to magnetized stars with inclined dipole geometry (Romanova et al. 2003, 2004; Kulkarni & Romanova 2005). In this paper we show more recent simulation results obtained with our “cubed sphere” grid.

¹Astronomy Department, Cornell University, Ithaca, NY 14853

²Institute for Mathematical Modeling of the Russian Academy of Sciences, Moscow, 125047, Russia

³Keldysh Institute of the Applied Mathematics of the Russian Academy of Sciences, Moscow, 125047, Russia

⁴Center for Theoretical Astrophysics, Dept. of Physics, University of Illinois at Urbana-Champaign, 1110 W. Green St., Urbana, IL 61801

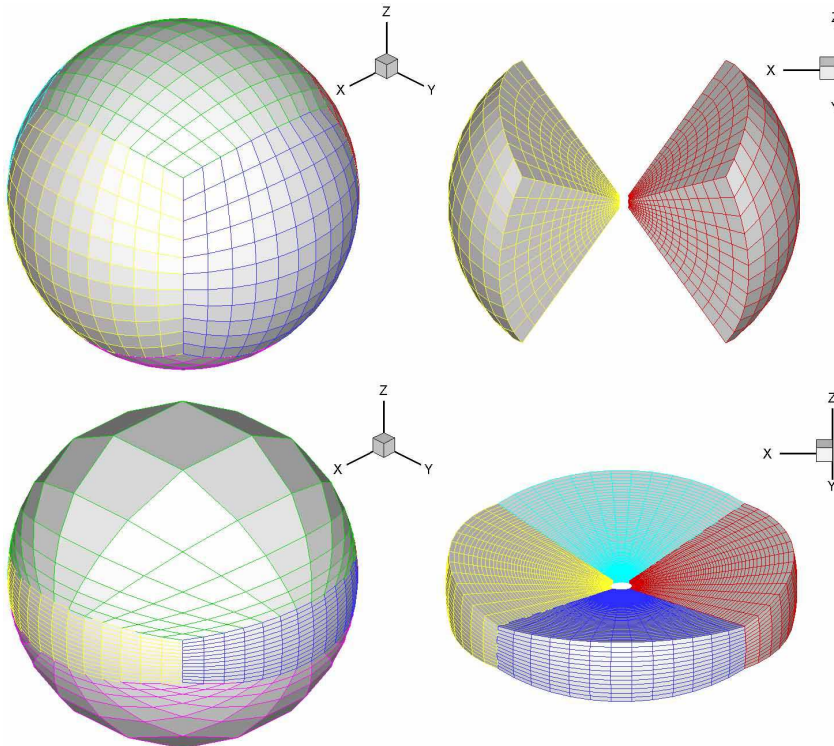


Figure 1. *Top*: cubed sphere grid used in simulations. The grid consists of 6 blocks corresponding to the 6 sides of a cube. *Bottom*: Cubed sphere grid with high resolution near the equator.

2. Numerical Method and “Cubed Sphere” Grid

We consider disk accretion to a rotating magnetized star. This problem is difficult to treat numerically because the magnetic field varies strongly with distance from the star ($\sim 1/R^3$ in case of the dipole field and even more steeply for higher multipoles), and it is rapidly varying in the laboratory inertial reference frame. To minimize errors in calculating the magnetic force, the magnetic field \mathbf{B} is decomposed into the “main” dipole component of the star, \mathbf{B}_0 , and the component \mathbf{B}_1 induced by currents in the disk and in the corona (Tanaka 1994). Another difficulty with this problem is that the dipole moment changes with time. It rotates with angular velocity $\boldsymbol{\Omega}$ so that the “main” field \mathbf{B}_0 also changes with time. Consequently, in the induction equation there is a large term involving \mathbf{B}_0 . To overcome this difficulty we use a coordinate system rotating with angular velocity $\boldsymbol{\Omega}$:

$$\begin{aligned} \partial\rho/\partial t + \nabla \cdot (\rho\mathbf{v}) &= 0, \\ \partial(\rho\mathbf{v})/\partial t + \nabla \cdot \mathbf{T} &= \rho\mathbf{g} + 2\rho\mathbf{v} \times \boldsymbol{\Omega} - \rho\boldsymbol{\Omega} \times (\boldsymbol{\Omega} \times \mathbf{R}), \\ \partial(\rho S)/\partial t + \nabla \cdot (\rho S\mathbf{v}) &= 0, \end{aligned}$$

$$\partial \mathbf{B} / \partial t = \nabla \times (\mathbf{v} \times \mathbf{B}),$$

where \mathbf{v} is velocity of plasma in the rotating frame, \mathbf{B} is the magnetic field, and S is the specific entropy. T is the stress tensor with components $T_{ik} \equiv p\delta_{ik} + \rho v_i v_k + (B^2\delta_{ik}/2 - B_i B_k)/4\pi + \tau_{ik}$. Here τ_{ik} is viscous stress, p is the gas pressure. We consider that the viscous stress is determined mainly by the gradient of the angular velocity because the azimuthal velocity is the dominant component in the disk. We use the α -viscosity model of Shakura and Sunyaev (1973) with the coefficient of dynamic viscosity $\eta_t = \alpha p / \Omega_K$, where α is a dimensionless coefficient, $\alpha < 1$. The viscosity acts only in the accretion disk so that the dominant contribution to the viscous stress arises from the gradient of the azimuthal velocity (approximately Keplerian) of the plasma. In cylindrical coordinates the non-zero components of the viscous stress tensor are

$$\tau_{r\phi} = \tau_{\phi r} = -\eta_t \frac{\partial \Omega_K}{\partial r} = \frac{3}{2} p,$$

where Ω_K is the Keplerian angular velocity at the given location. We calculate momentum fluxes due to the viscous stress at faces of the grid after transforming to the Cartesian coordinates.

The ‘‘Cubed Sphere’’ Grid. The three dimensional grid consists of a set of concentric spheres of radii R_j in a geometric progression with $j = 1..N_R$. The grid on the surface of the sphere consists of six sectors with the grid on each sector topologically equivalent to the equidistant grid on the face of a cube. In each sector the grid of $N \times N$ cells is formed by the arcs of great circles separated by equal angles. This grid gives high spatial resolution close to the star which is important for our study. Recently we incorporated the option to allow the grid to be compressed towards the equatorial plane, to have higher grid resolution in the disk (Fig. 1, bottom plots). Such a grid is needed when higher resolution is required in the disk. Typical grid resolutions used in our simulations vary from $N_R \times N^2 = 72 \times 31^2$ cells in each of the six sectors, up to $N_R \times N^2 = 288 \times 121^2$ depending on the problem. The cubed sphere grid naturally lends itself to division into $6 \times N$ regions (with N cuts in the radial direction), which are calculated in parallel using from 48 up to 240 processors.

Godunov-Type Finite-Difference Scheme. All variables are evaluated at the centers of the cells, and all vector variables are expressed in terms of their Cartesian components. Finite difference equations are written for the Cartesian components of vector variables. The finite difference scheme of Godunov’s type has the form:

$$\frac{\mathcal{U}^{p+1} - \mathcal{U}^p}{\Delta t} V + \sum_{m=1..6} s_m \mathcal{F}_m = \mathcal{Q}.$$

Here, $\mathcal{U} = \{\rho, \rho \mathbf{v}, \mathbf{B}, \rho S\}$ is the ‘‘vector’’ of the densities of conserved variables; \mathcal{F}_m is the ‘‘vector’’ of flux densities normal to the face ‘‘ m ’’ of the grid cell, s_m is the area of the face ‘‘ m ’’, V is the volume of the cell, \mathcal{Q} is the intensity of sources in the cell, and Δt is the time step. To calculate the flux densities \mathcal{F}_m , an approximate Riemann solver is used, analogous to the one described by Powell *et al.* (1999) and by Kulikovskii *et al.* (2001).

3. Accretion in stable and unstable regimes

One of the most striking recent results obtained in our group is the discovery of accretion through the interchange instability (Kulkarni & Romanova 2008; Romanova et al. 2008). Simulations have shown that a magnetized star may be either in the stable or unstable regime of accretion. In the stable regime matter accretes to the star in two ordered funnel streams and produces ordered hot spots on the surface of the star, leading to periodic light curves (see Fig. 2, left panels). In the unstable regime matter penetrates through the magnetosphere due to the interchange instability forming a small number (2 to 7) of “tongues” (see also Li & Narayan 2004) which form chaotically at different parts of the inner disk, and the light-curve from the resulting stochastic hot spots is expected to be irregular (see Fig.2, right panels).

There are a number of factors which determine the regime of accretion. If the magnetic axis is inclined with the rotation axis at a large enough angle, $\Theta > 30^\circ$, then the flow is usually stable (Kulkarni & Romanova 2009). If the inclination is small, e.g., $\Theta = 5^\circ$ (used in the majority of our simulations), then the stability of accretion depends on various other factors.

We compared our simulations with a few relevant theoretical approaches. The basic theory states that a homogeneous vertical field at the disk-magnetosphere boundary does not damp azimuthal perturbations, and therefore is not an obstacle for the development of unstable ϕ -modes (e.g. Arons & Lea 1976). A more general criterion for magnetized accretion disks states that the disk is unstable to growth of ϕ -modes if $\gamma_{B\Sigma}^2 \equiv -g_{eff} d\ln(\Sigma/B_z)/dr > 2(r_m d\Omega/dr)^2 \equiv \gamma_\Omega^2$ (e.g. Spruit, Stehle & Papaloizou 1995; see also Kaisig, Tajima & Lovelace 1992). Here, $-g_{eff} = r(\Omega_K^2 - \Omega^2)$ is the effective gravity, and $\Sigma = 2\rho h$ is the surface density. That is, for the instability to start, the surface density per unit magnetic field strength Σ/B_z should drop off fast enough in the direction of the star, that the term $\gamma_{B\Sigma}^2$ is larger than the term associated with the shear, γ_Ω^2 , which tends to suppress the instability by smearing out the perturbations. In addition the term $-g_{eff}$ should be large enough and positive for the instability to start. In one set of runs we fixed rotation rate of the star and the initial surface density in the disk and varied the accretion rate by varying the α -parameter: $\dot{M} \sim \Sigma v_r \sim \alpha$. We observed that cases with $\alpha < 0.04$ (small \dot{M}) correspond to stable accretion, while cases with $\alpha > 0.04$ (large \dot{M}) correspond to unstable accretion. We observed that at larger \dot{M} , the gradient $d\ln(\Sigma/B_z)/dr$ is larger and the shear $2(r_m d\Omega/dr)^2$ is smaller. In addition, at larger \dot{M} the inner disk comes closer to the star, which increases $-g_{eff}$. All these factors make instability more favorable. Thus, we observed that increasing in accretion rate leads to transition from the stable to the unstable regime (Kulkarni & Romanova 2008; Romanova et al. 2008). In another set of runs we fixed the accretion rate in the disk by fixing α at some small value, $\alpha = 0.02$, but varied the rotation rate of the star Ω . We observed that at low stellar rotation rates the flow is unstable, while at higher rates it becomes stable. This is ascribed to the decrease in the effective gravity, $-g_{eff}$, by fast rotation. The accretion is stabilized when the star is spun up and the effective gravity is reduced to a certain point (Kulkarni & Romanova 2009). The first effect, namely, the dependence of the state (stable or unstable) on the accretion rate \dot{M} , may have important observational

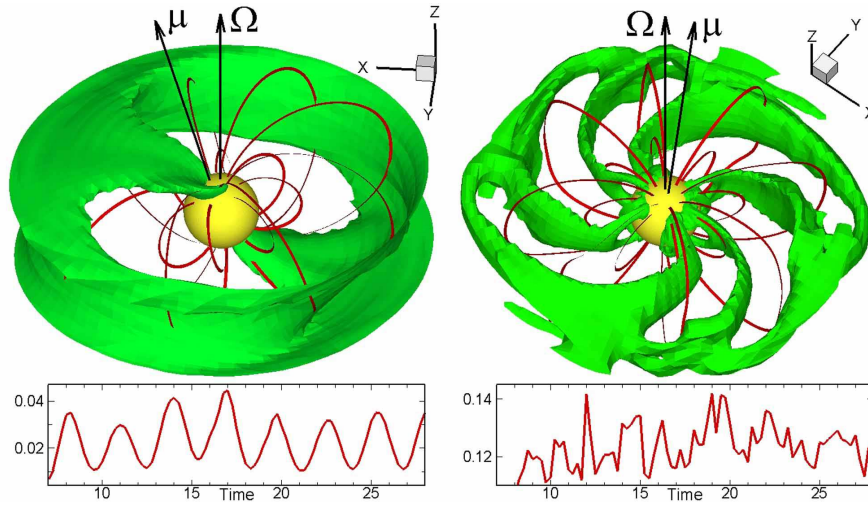


Figure 2. *Left:* Accretion in stable regime. The surface is a constant density surface, and the lines are sample magnetic field lines. The magnetic axis of the dipole μ is inclined relative to the rotational axis Ω at $\Theta = 15^\circ$. *Right:* Accretion in the unstable regime at $\Theta = 5^\circ$ (from Romanova, Kulkarni & Lovelace 2008).

consequences: a particular star may transition between these two regimes and may thus show intermittency of pulsations. The effect of intermittency has been observed in a few millisecond pulsars (e.g. Altamirano et al. 2008). This discovery greatly changes our understanding of accreting magnetized stars and their possible observational properties.

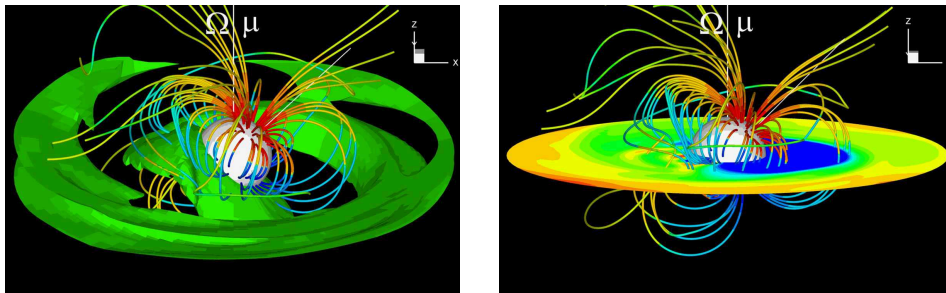


Figure 3. *Left:* Accretion to a star with a dipole ($\Theta = 45^\circ$) and a quadrupole ($\Theta_D = 30^\circ$) magnetic field (of comparable amplitudes near the star) misaligned at $\Phi = 90^\circ$. A constant density surface and magnetic field lines are shown. *Right:* Same as in the left panel, but showing density contours in the equatorial plane (from Long, Romanova & Lovelace 2008).

4. Accretion to a star with complex magnetic field

The stellar magnetic field may be more complex than dipole (e.g., Donati et al. 2007). As a first step we investigated accretion to a star with mixed dipole and quadrupole fields:

$$\mathbf{B}(\mathbf{r}) = \frac{3(\boldsymbol{\mu} \cdot \hat{\mathbf{r}})\hat{\mathbf{r}} - \boldsymbol{\mu}}{r^3} + \frac{3D}{4r^4}(5(\hat{\mathbf{D}} \cdot \hat{\mathbf{r}})^2 - 1)\hat{\mathbf{r}} - \frac{3D}{2r^4}(\hat{\mathbf{D}} \cdot \hat{\mathbf{r}})\hat{\mathbf{D}},$$

where $\boldsymbol{\mu}$ is the dipole moment, \mathbf{D} is the quadrupole moment, and $\hat{\mathbf{r}}$ and $\hat{\mathbf{D}}$ are the unit vectors for the position and the quadrupole moment respectively. In general, the dipole and quadrupole moments $\boldsymbol{\mu}$ and \mathbf{D} are misaligned relative to the rotational axis $\boldsymbol{\Omega}$, at angles Θ and Θ_D respectively. In addition, they can be in different meridional planes with an angle Φ between the $\boldsymbol{\Omega} - \boldsymbol{\mu}$ and $\boldsymbol{\Omega} - \mathbf{D}$ planes. First, we investigated the case when the moments are aligned with each other but not with the rotational axis. We found that in this case, a significant amount of matter may flow through the “quadrupole belt” forming a ring-shaped spot on the surface of the star (Long et al. 2007). In the more general case when the dipole and quadrupole moments are not in the same plane, the field is more complicated with a number of poles of different polarity on the surface of the star (Long et al. 2008). The accreting matter chooses the most energetically favorable path, due to which the funnel streams are often quite close to the equatorial plane (see Fig. 3). Work on accretion to a star with a higher multipolar field is in progress.

Acknowledgments. The authors were supported in part by NASA grant NNX08AH25G and by NSF grants AST-0607135 and AST-0807129. MMR is thankful to NASA for using NASA High Performance Facilities. AVK and GVV were supported in part by grant RFBR 06-02016608, Program 4 of RAS. MMR and RVEL thank the organizers for a very interesting meeting.

References

- Altamirano, D., Casella, P., Patruno, A., Wijnands, R., & van der Klis, M., ApJ, 674, L45
- Arons, J., & Lea, S.M. 1976, ApJ, 207, 914
- Bouvier, J., Alencar, S.H.P., Harries, T.J., Johns-Krull, C.M., & Romanova, M. M. 2007, Protostars and Planets V, B. Reipurth, D. Jewitt, and K. Keil (eds.), University of Arizona Press, Tucson, p.479
- Donati J.-F., Jardine, M.M., Gregory, S.G., et al. 2007 MNRAS, 380, 1297
- Kageyama, A., & Sato, T. 2004, Geochem. Geophys. Geosyst. 5 doi: 10.1029/2004GC000734
- Kaisig, M., Tajima, T., & Lovelace, R. V. E. 1992, Astroph. J. 386, 83
- Koldoba, A.V., Romanova, M.M. , Ustyugova, G.V., & Lovelace, R.V.E. 2002, ApJ, 576, L53
- Kulikovskii, A. G., Pogorelov, N. V., & Semenov, A. Y. 2001, Mathematical Aspects of Numerical Solution of Hyperbolic Systems (Boca Raton: Chapman & Hall)
- Kulkarni, A.K. & Romanova, M.M. 2005, ApJ, 633, 349
- Kulkarni, A.K. & Romanova, M.M. 2008, MNRAS, 386, 673
- Kulkarni, A.K. & Romanova, M.M. 2009, MNRAS, in press
- Li, L.-X. & Narayan, R. 2004, Astroph. J. 601, 414
- Long, M., Romanova, M.M., Lovelace, R.V.E. 2007, MNRAS, 374, 436,

- Long, M., Romanova, M.M., Lovelace, R.V.E. 2008, MNRAS, 386, 1274
- Powell, K.G., Roe, P.L., Linde, T.J., Gombosi, T.I., & De Zeeuw, D.L. 1999, J. Comp. Phys., 154, 284
- Putman, W.M., & Lin, S.-J. 2007, J. Comp. Phys., 227, 55
- Romanova, M.M., Kulkarni, A.K., Lovelace, R.V.E. 2008, ApJ Letters, 673, L171
- Romanova, M.M., Ustyugova, G.V., Koldoba, A.V., Wick, J.V., & Lovelace, R.V.E. 2003, ApJ, 595, 1009
- Romanova, M.M., Ustyugova, G.V., Koldoba, A.V., & Lovelace, R.V.E. 2004, ApJ, 610, 920
- Ronchi, C., Iacono, R., & Paolucci, P.S. 1996, J. Comp. Phys. 124, 93
- Sadourny, R. 1972, Mon. Weather Rev., 100, 136
- Shakura, N.I., & Sunyaev, R.A. 1973, A&A, 24, 337
- Spruit, H. C., Stehle, R., & Papaloizou, J.C.B. 1995, A&A, 229, 475
- Tanaka, T. 1994, J. Comp. Phys., 111, 381